

The Group Evolution Multiwavelength Study (GEMS): bimodal luminosity functions in galaxy groups

Trevor A. Miles¹*, Somak Raychaudhury¹, Duncan A. Forbes², Paul Goudrooij³, Trevor J. Ponman¹ & Vera Kozhurina-Platais³

¹School of Physics and Astronomy, The University of Birmingham, Birmingham B15 2TT, UK

²Centre for Astrophysics and Supercomputing, Swinburne University, Hawthorn, VIC 3122, Australia

³Space Telescope Science Institute, 3700 San Martin Drive, Baltimore, MD 21218

MNRAS accepted - 2004 August

ABSTRACT

We present B and R -band luminosity functions (LF) for a sample of 25 nearby groups of galaxies. We find that the LFs of the groups with low X-ray luminosity ($L_X < 10^{41.7}$ erg s $^{-1}$) are significantly different from those of the X-ray brighter groups, showing a prominent dip around $M_B = -18$. While both categories show lack of late-type galaxies in their central regions, X-ray dim groups also show a more marked concentration of optical luminosity towards the centre. A toy simulation shows that in the low velocity dispersion environment, as in the X-ray dim group, dynamical friction would facilitate more rapid merging, thus depleting intermediate-luminosity galaxies to form a few giant central galaxies, resulting in the prominent dip seen in our LFs. We suggest that X-ray dim (or low velocity dispersion) groups are the present sites of rapid dynamical evolution rather than their X-ray bright counterparts, and may be the modern precursors of fossil groups. We predict that these groups of low velocity dispersion would harbour younger stellar populations than groups or clusters with higher velocity dispersion.

Key words: galaxies: luminosity functions — galaxies: evolution — galaxies: structure — galaxies: groups

1 INTRODUCTION

Galaxy luminosity functions (LF) provide a means of comparison between the populations of galaxies of various luminosities in different environments, and contain valuable information about the physical processes that feature prominently in galaxy formation. Models of galaxy formation have been related to observable luminosity functions of galaxy populations from the basic principles of White & Rees (1978) to more recent detailed models including stellar evolution, merging, cooling and feedback (White & Frenk 1992; Cole et al. 1994; Somerville & Primack 1999; Kauffmann et al. 1999; Benson et al. 2003). These models are now being put to the test by high-quality photometric observations of wide-field and deep samples of the field and in highly clustered regions.

Early researchers, such as Turner & Gott (1976), motivated by the potential usefulness of the LF as a distance indicator, accepted the paradigm that all ensembles of galaxies, from groups to rich clusters, follow a Universal luminosity function. The shape of this luminosity function is usually modelled as (Schechter 1976)

$$\phi(L) = (\phi^*/L^*)(L/L^*)^\alpha e^{-L/L^*}. \quad (1)$$

The Schechter function drops sharply at bright magnitudes and rises at the faint end following a power law of slope α , the transition occurring around the luminosity L^* , ϕ^* being the normalisation parameter. Field samples usually yield $\alpha = -1.0$ (e.g., APM-Stromlo, Loveday et al. 1995, b_J -band), but shallower or steeper slopes have been found (e.g., LCRS, Lin et al. 1996, R -band, $\alpha = -0.7$; 2dF, Madgwick et al. 2002, b_J -band, $\alpha = -1.19$).

However, accurate photometry of the faint end of the LF reveals that the LF may be more complex, and features such as dips at intermediate luminosities or an excess of faint galaxies are sometimes found, making a single Schechter function a poor fit to the data. Hunsberger et al. (1998) find a dip at $M_R = -18$ in the composite LF of 37 Hickson compact groups (HCG), an effect which has been found at brighter magnitudes in a few rich clusters of galaxies (e.g. Abell 2554, Coma) by various other studies (e.g. Trentham & Tully 2002; Smith et al. 1997). Indeed, there has been a recent move towards modelling the LF of brighter galaxies ($M_B < -18.5$) as Gaussian, and that of the fainter ones with a Schechter function (e.g. Lobo et al. 1997; Andreon & Pelló 2000). This approach seeks to explain the peaks and dips in the LF as due to a varying mix of galaxies of different morphological types in different environments, and highlights the connection be-

* E-mail: tm@star.sr.bham.ac.uk

tween the evolution of galaxies and their local environment (e.g. Ferguson & Sandage 1991; Jerjen 2001).

Furthermore, there has been a lack of consensus about the overall shape of the LF in groups of galaxies. Zabludoff & Mulchaey (2000) found that the LF of X-ray bright groups shows an excess of faint galaxies, with a Schechter index of $\alpha = -1.3 \pm 0.1$, while Mendes de Oliveira & Hickson (1991) find evidence of depletion of faint galaxies $\alpha = -0.2 \pm 0.1$ in HCGs. Zepf et al. (1991) find an intermediate value of $\alpha = -1.0 \pm 0.1$, similar to that in the field, in 17 HCGs, while Hunsberger et al. (1998) find a slight excess of dwarf galaxies when compared to the field ($\alpha = -1.17 \pm 0.1$) in 37 HCGs. A possible source of the anomalies between these studies is the subtraction of the extragalactic background, which is sensitive to inhomogeneities in the large-scale structure, and lack of information of group membership, which is in principle redeemable with redshift measurements.

Here we suggest that where sufficient redshift and colour information is available, categorising the LF of groups of galaxies in terms of X-ray luminosity (or equivalently, group velocity dispersion, e.g., Helson & Ponman (2000)) is an effective method for investigating the connection between differences in the shapes of group luminosity functions and the local environment, and probing the underlying galaxy populations and history of evolution.

In the following section, we present observations of 25 groups of galaxies, and in §3, compute their luminosity function in the *B* and *R*-band, splitting the sample in categories based on their X-ray luminosity. In §4, we use toy-model simulations to qualitatively explain the differences in the LFs of X-ray bright and dim groups, and in §5, we discuss the implications in the context of the evolution of galaxies in groups. We have used $H_0 = 70 \text{ km s}^{-1}\text{Mpc}^{-1}$; $q_0 = 0.5$ throughout.

2 OBSERVATIONS AND ANALYSIS

Our sample of 25 groups is drawn from the Group Evolution Multi-wavelength Study (Osmond & Ponman 2004, GEMS) of sixty groups of galaxies, compiled to incorporate a wide variety of groups representing a wide range of evolutionary stage and local environment. The master sample was compiled by cross-correlating a list of over 4000 catalogued groups with archival ROSAT PSPC X-ray observations with integration >10 ks. A large fraction of these were detected in the X-ray, and for the others we have upper limits for their X-ray flux.

2.1 Photometry and calibration

Of this sample, 17 groups were observed at the 2.5m Isaac Newton telescope at the Roque de Los Muchachos Observatory, La Palma, between 2000 February 4–10. The detector used was the prime focus Wide Field Camera (WFC), which is an array of four thinned EEV CCDs, each with an area of 2048×4096 pixels, each 0.33 arcsec across. Each CCD thus can image an area of 22.5×11.3 arcmin of sky, together covering 1017 sq.arcmin. Images obtained with broadband BVI filters were processed using standard NOAO IRAF packages.

A further 8 groups were observed with the 2.2m ESO/MPI telescope at La Silla observatory using the Wide Field Imager (WFI), between 2001 August 7–10. The WFI is a focal reducer-type mosaic camera with 8 CCD chips each with 2048×4098 pixels, the pixel scale is 0.238 arcsec providing a field of view for the

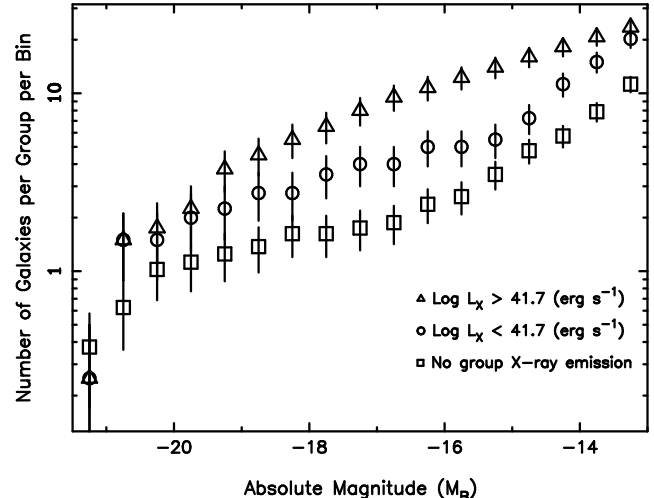


Figure 1. The Cumulative *B*-band Luminosity Function for 25 groups of galaxies separated into three categories: X-ray bright groups (triangles), X-ray dim (circles) and X-ray undetected groups (those with no discernible group emission, squares). It is clear that the LF of the X-ray bright groups is different from that of the other two classes, the latter showing a “dip” between $-19 < M_B < -17$. We combine the X-ray dim and undetected groups into a single category in the rest of the paper.

whole camera of 34×33 arcmin. Photometry was performed with broadband BRI filters. Exposures of standard star fields (Landolt 1992) were taken during both observing sessions. The ESO images were reduced using the ESOWFI package implemented within IRAF (Jones & Valdes 2000).

The average integration times used per image were 780s in the *B*-band, 390s in the *R*-band and 290s in the *I*-band for the INT run, and 600s in the *B*-band, 300s in the *R*-band and 180s in the *I*-band for the ESO run. The median seeing achieved throughout the run was between 1.2 arcsec FWHM in the *B* filter, 1.1 arcsec in *R* and 1.0 arcsec in *I* measured from the brightest unsaturated stars in the field for INT observations and 1.3 arcsec in the *B* filter, 1.1 arcsec in *R* and 0.9 arcsec in *I* for ESO observations.

2.2 Galaxy Selection

Images were identified and fluxes extracted using the SExtractor package (Bertin & Arnouts 1996). For all identified objects, positions, magnitudes, fluxes, star/galaxy classifiers and flags were written to a catalogue. The “stellaricity” parameter uses a neural network-based algorithm to classify images. Detections were checked visually and objects with stellaricity > 0.9 were deemed to be definitely stellar and therefore not subject to further analysis. All objects with FWHM less than the PSF were discarded as noise. All galaxies identified by this procedure were visually inspected, and classified as early (E/S0) or late (S/Irr) types.

A fixed aperture, set to be slightly greater than the seeing, was used to obtain magnitudes in all filters for colour selection. Objects in different filters were matched and aperture magnitudes were subtracted to find colours.

Galaxies were selected as being likely group members on the basis of their $(B - R)$ colour. A cut-off was selected at $(B - R) = 1.7$ for all groups, which represents a conservative selection criterion and removes the majority of background galaxies. This selection criterion was chosen on the basis of the work of Fukugita et al. (1995), where, using colours of galaxies at various redshifts, ob-

Table 1. The sample of groups of galaxies used in this study

Group	R.A. J2000	Dec J2000	Obs. ^a	Distance ^b Mpc	σ km/s	$\log L_X$ ergs/s ^c	Emission ^d Type
NGC 524	01:24:47.8	+09:32:19	I	35.4	175	41.05	Galaxy
HCG 10	01:26:07.4	+34:41:27	I	68.2	231	41.70	Group
NGC 720	01:53:00.4	-13:44:18	E	23.2	273	41.20	Group
NGC 1052	02:41:04.8	-08:15:21	I	20.3	91	40.08	Galaxy
HCG 22	03:03:31.0	-15:41:10	E	38.7	25	40.68	Group
NGC 1332	03:26:17.1	-21:20:05	E	22.9	186	40.81	Galaxy
NGC 1566	04:20:00.6	-54:56:17	E	20.8	184	40.41	Galaxy
NGC 1587	04:30:39.9	+00:39:43	I	55.2	115	41.18	Group
NGC 2563	08:20:35.7	+21:04:04	I	73.5	384	42.50	Group
NGC 3227	10:23:30.6	+19:51:54	I	26.5	169	41.23	Galaxy
NGC 3396	10:49:55.2	+32:59:27	I	31.2	106	40.53	Galaxy
NGC 3607	11:16:54.7	+18:03:06	I	23.5	280	41.05	Group
NGC 3640	11:21:06.9	+03:14:06	I	28.5	211	<40.37	Undetected
NGC 3665	11:24:43.4	+38:45:44	I	37.2	87	41.11	Group
NGC 4151	12:10:32.6	+39:24:21	I	23.0	102	<40.20	Undetected
NGC 4261	12:19:23.2	+05:49:31	I	41.2	197	41.92	Group
NGC 4636	12:42:50.4	+02:41:24	I	10.3	284	41.49	Group
NGC 4725	12:50:26.6	+25:30:06	I	25.1	49	40.63	Galaxy
NGC 5044	13:15:24.0	-16:23:06	I	33.2	426	43.01	Group
NGC 5322	13:49:15.5	+60:11:28	I	34.9	166	40.71	Galaxy
HCG 68	13:53:26.7	+40:16:59	I	41.1	191	41.52	Group
NGC 5846	15:06:29.2	+01:36:21	E	29.9	346	41.90	Group
NGC 7144	21:52:42.9	-48:15:16	E	26.6	41	40.33	Galaxy
HCG 90	22:02:08.4	-31:59:30	E	36.3	131	41.49	Group
IC 1459	22:57:10.6	-36:27:44	E	25.6	223	41.28	Group

^a Observations obtained at (I) the INT, La Palma and (E) the 2.2m ESO/MPI telescope

^b Distance measured from the redshift of central galaxy (assuming $H_0 = 70 \text{ km s}^{-1}\text{Mpc}^{-1}$; $q_0 = 0.5$), corrected for local bulk flows.

^c Bolometric X-ray luminosity from Osmond & Ponman (2004)

^d “Group” emission refers to unambiguous detection of diffuse X-ray emission from hot gas in the group potential, not belonging to any galaxy. Those marked “Galaxy” have no discernible diffuse emission that doesn’t belong to individual galaxies, and those “undetected” fall below the detection threshold of the ROSAT PSPC observation used.

tained in 48 photometric bands, it was shown that all elliptical galaxies with $(B - R) > 1.7$ have a redshift greater than 0.2. The most distant group in our present sample has a redshift of $z = 0.016$ (NGC 2563 group).

Distances to the groups were calculated from redshifts, by estimating peculiar velocities according to a model of the local velocity field, including the infall into Virgo and the Great Attractor (for further details, see Osmond & Ponman (2004)).

2.3 Background Subtraction

Given that the number of galaxies belonging to each group is small, a major reason for disagreement between various authors as to the nature of the galaxian LF in groups is that the number of background and foreground galaxies seen in each group in projection can be rather significant.

Flint *et al.* (2001) point out that while a system of classification by colour, like ours, is appropriate for the majority of galaxy types, there exists a population of very red ($B - R > 1.7$), low surface brightness galaxies which may be misclassified as background objects. On the other hand, high-resolution HST photometry of the elliptical galaxies IC4051 and NGC4481 in Coma (Andreon & Cuillandre 2002) has revealed blends of globular clusters that were classified as single extended sources from the ground, which caused significant contamination of the faint end of the lu-

minosity function in the Coma cluster at $R \gtrsim 21$. However, since the average distance modulus of our groups is ~ 33 (as opposed to 35 for Coma), and we compute LFs down to $M_B = -13$, we expect contamination from blends of globular clusters to be minimal.

Having tried various processes of background subtraction, we chose to evaluate the luminosity function of all galaxies with $B - R < 1.7$ from the regions outside a radius of R_{500} from the centre of the group (values from Osmond & Ponman 2004) and use it as the background for subtraction.

3 THE LUMINOSITY FUNCTION OF GALAXIES IN GROUPS

The galaxian luminosity function (LF) of the groups is evaluated here by co-adding galaxies of the same absolute luminosity of several groups, since the number of member galaxies in each individual group is small. The groups in our sample represent very diverse systems in terms of their content and physical properties. We therefore chose to assemble the galaxies according to the X-ray luminosity of their parent groups, which provides a measure of the mass and velocity dispersion of the group, and helps to distinguish between virialised systems and dynamically young and forming systems. We use the X-ray luminosities measured by Osmond & Ponman (2004), who used ROSAT PSPC observations in the 0.5–2 keV

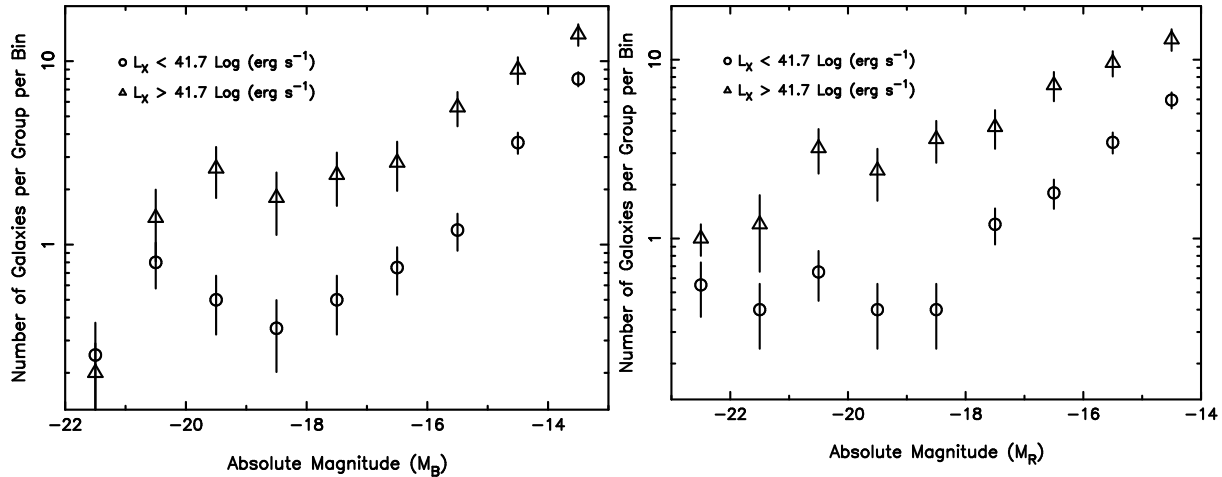


Figure 2. Differential *B*-band (left) and *R*-band (right) Luminosity Function of 25 GEMS Groups of galaxies: X-ray bright groups ($L_X > 10^{41.7} \text{ erg s}^{-1}$, triangles) and X-ray dim groups ($L_X < 10^{41.7} \text{ erg s}^{-1}$, circles). It is clear that the LF of the dim groups show a “dip” in the LF between $-19 < M_B < -17$ and $-20 < M_R < -18$. The bright groups too show dips, albeit not so pronounced, in the same intervals.

range, fitting β -profiles after point source removal, extrapolated to estimate the bolometric X-ray luminosity.

We characterised the parent groups as X-ray bright if their bolometric X-ray luminosity is more than the median of the sample, $L_X = 10^{41.7} \text{ erg s}^{-1}$, and X-ray dim if less. This X-ray luminosity refers to that of the group plus any central galaxy that might exist. In addition, we add a third category (“X-ray undetected” groups) where there is no discernible group emission, and all the diffuse emission, if any, can be accounted for by emission from individual non-central galaxies in the group.

The cumulative galaxian Luminosity Function (*B*-band) of the 25 GEMS Groups in our sample, separated into the three categories described above (X-ray bright, dim and undetected), and plotted for all galaxies together in each category, is shown in Fig. 1. A clear difference between the X-ray bright groups and those in the other two categories is immediately evident, with a depletion or ‘dip’ in the number of galaxies with magnitudes between $-19 < M_B < -17$ for the latter. In the cumulative LF, as is plotted in Fig. 1, this shows up as a flat region in the above magnitude range.

The possibility that this dip is due to some of the galaxies being systematically missed can be ruled out, as we are complete to over five magnitudes dimmer than the position of the dip. According to the Poisson statistics used to calculate the error bars, we can also reject the hypothesis that a statistical fluctuation accounts for the differences between the groups.

3.1 X-ray bright and dim groups

There is no significant difference, as revealed by the Kolmogorov-Smirnov (KS) test, between the shape of the luminosity functions of the X-ray dim and the X-ray undetected groups (circles and squares in Fig. 1). Therefore, for the rest of the paper we will combine them into a single category of X-ray dim groups.

The LFs of the groups of Fig. 1 are now re-plotted into two categories of X-ray bright ($L_X > 10^{41.7} \text{ erg s}^{-1}$) and dim (those that have lower X-ray luminosity). The differential *B*-band and *R*-band luminosity functions are plotted in Fig. 2. The null hypothesis that the two distributions were drawn from the same population was rejected at the 99.999% level of confidence for both LFs shown in Fig. 2. These LFs clearly show the position of the dip for the X-ray

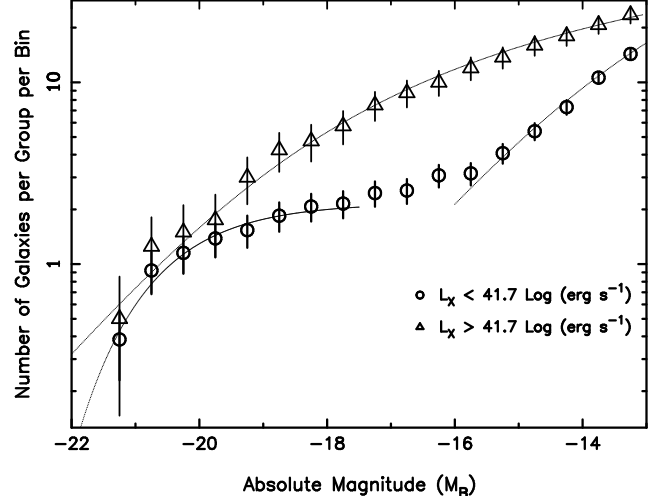


Figure 3. Cumulative *B*-band Luminosity Function of 25 GEMS Groups of galaxies grouped into the same categories as 2 The former is fit with a single Schechter function, whereas the superposed curve on the latter represent two Schechter functions.

dim groups, between $-19 < M_B < -17$ and $-20 < M_R < -18$ respectively. Interestingly, the X-ray bright group LFs also show a slight dip in the same interval, though by far not as prominently, such that it is not easily apparent from the corresponding cumulative LF (*B*-band only, Fig. 3).

We fit the luminosity function of X-ray bright groups with a single Schechter function of the form (1), yielding best fit values in the *B*-band of $M^* = -20.1 \pm 0.1$ and $\alpha = -1.04 \pm 0.01$, with the reduced χ^2 for the fit being 0.9. It is clear that the LF of the X-ray dim groups in Fig. 2 is not well-fit by a single smooth function: an attempt to fit it by a single Schechter function yielded a reduced χ^2 of 54. If we fit the LF in this category with two Schechter functions, we obtain, for the bright end, $M^* = -20.5 \pm 0.1$ and $\alpha = -0.04 \pm 0.01$, whereas for the faint end, the best fit yields $M^* = -14.0 \pm 0.1$ and $\alpha = -1.01 \pm 0.01$.

Fig. 4 shows the differential and cumulative *B*-band LFs separately for early-type and late-type galaxies, for both X-ray bright and faint parent groups. The LF of early-type galaxies shows a

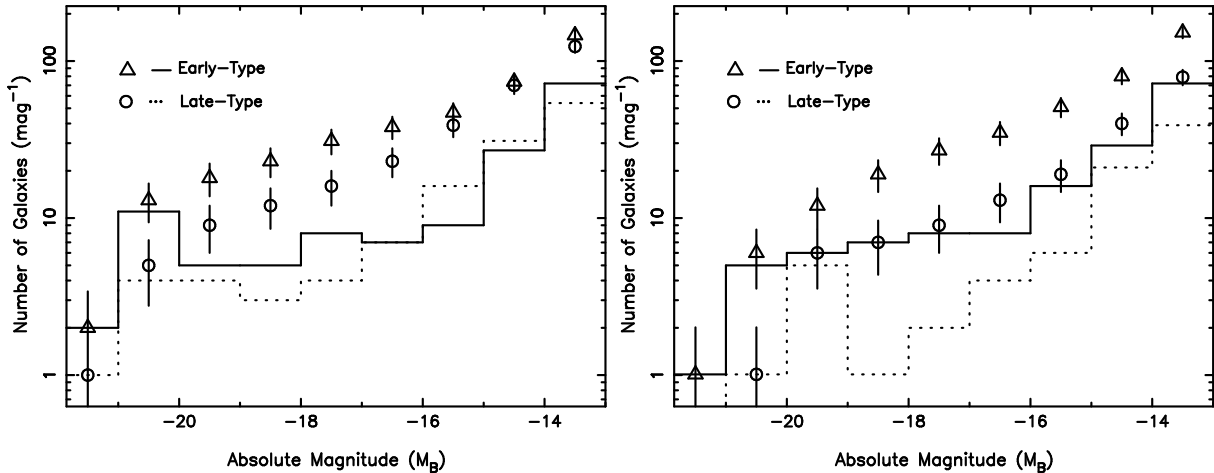


Figure 4. B -band luminosity functions for early and late-type galaxies for the X-ray dim (left) and bright (right) groups. The histograms show the differential LFs (solid: early, dotted: late), whereas the points represent the cumulative LFs (triangles: early, circles: late).

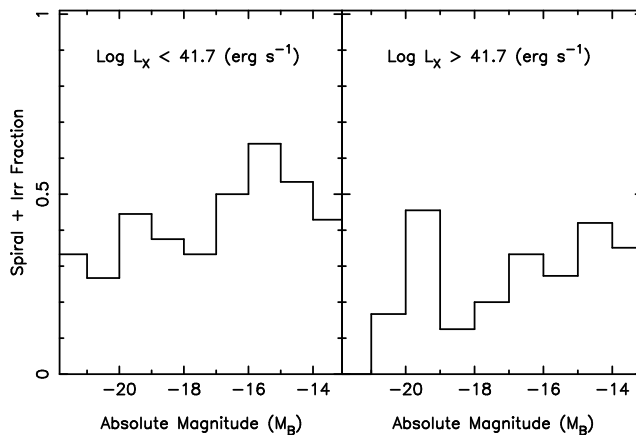


Figure 5. The fraction of late-type galaxies as a function of absolute magnitude, for the X-ray dim (left) and bright (right) groups. The X-ray dim groups have a lower fraction of late-type galaxies at the bright end.

significant dip in the X-ray dim systems, where there is none for the brighter systems (right panel). Even though the LF of late-type galaxies seems to have a peak at the bright end for the X-ray bright groups, the small numbers involved (Fig. 5) make the errors on each point considerably large and the brighter end of the late-type LF rather unreliable for these systems.

3.2 The radial distribution of galaxy light

Having looked at the relative distribution of galaxies of different luminosities in the group as a whole, we now turn to the distribution of light as a function of distance from the centre of each group. The centre and overdensity radius R_{500} for each group are taken from Osmond & Ponman (2004). The total blue light within the same scaled (projected) radius $R/R_{500} = 0.3$ is lower, and more centrally peaked, in X-ray dim groups than in X-ray bright groups (Fig. 6), suggesting that the groups in the former category are dynamically evolving.

The average number of bright ($M_B < -17$) early and late-type galaxies is plotted as a function of radial distance in Fig. 7. Both the X-ray bright and dim groups show a distribution of early-type galaxies that is centrally concentrated, though the X-ray dim

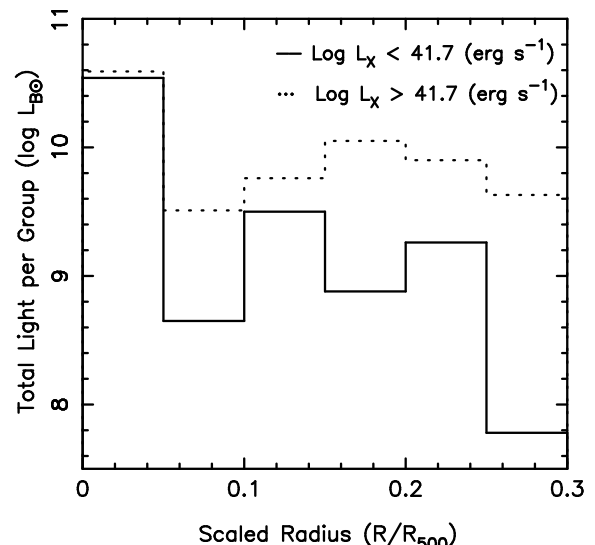


Figure 6. The mean B luminosity of all galaxies in high L_X and low L_X groups as a function of radius (expressed in terms of the standard radius R_{500} , determined from the group temperature). The luminosity within the same scaled projected radius $R/R_{500} = 0.3$ is lower in X-ray dim groups (solid histogram) than in X-ray bright groups (dotted histogram), suggesting that the latter are closer to a stage of virialisation.

groups display a far more centrally peaked distribution of galaxies than their X-ray bright counterparts. A KS test shows that the null hypothesis of the two distributions being drawn from the same sample is rejected at the 99.98% level of confidence. This is consistent with the observation that late-type galaxies tend to avoid the central regions of both kinds of groups, in addition to being rare in X-ray bright ones (as seen in Fig. 5).

3.3 Comparison with the Coma Cluster and the Leo I group

To compare our LFs with those of other studies, photometric images were obtained of the Coma Cluster and the Leo I group, during the same INT observing run as the Northern GEMS groups and with the same instrumental setup, in 2000 February.

We plot the differential R -band luminosity function for the

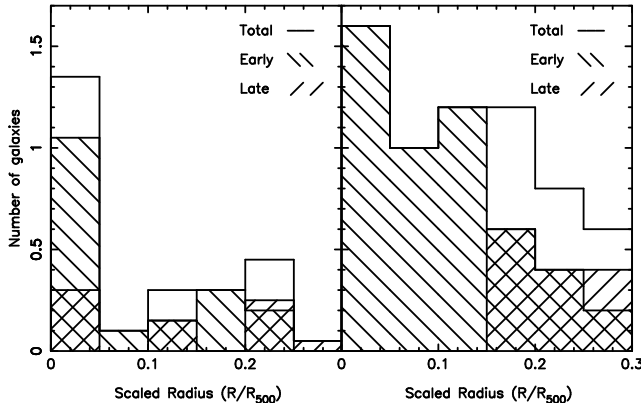


Figure 7. Average number of bright ($M_B < -17$) early and late-type galaxies, plotted as function of scaled projected radius, in (left panel) X-ray dim groups and (right panel) X-ray bright groups respectively. Both categories of group show a distribution that is centrally concentrated, and a lack of late-type galaxies in the central regions. However, the X-ray dim groups display a more centrally peaked distribution of early-type galaxies than their X-ray bright counterparts.

Coma cluster, following colour selection of member galaxies as above, in Fig. 8. The background subtraction employed here is a scaled (by relative area) version of that used by Secker et al. (1997), to facilitate direct comparison. The result is consistent with the Secker et al. (1997) LF within the errors. Small differences can be explained by the fact that we use different regions of the Coma cluster (which could be significant, as found by Beijersbergen et al. (2002)), and the membership criteria applied are slightly different.

Our Coma LF looks reassuringly similar to that of Secker et al. (1997), and reveals a shallow dip reminiscent of the X-ray bright GEMS groups, albeit in the slightly brighter absolute magnitude range $-20 < M_B < -18$. Similar dips have been observed in other individual rich clusters (e.g. Abell 2554, Smith et al. 1997), though it does not seem to be a common property of the luminosity functions of rich clusters, as is apparent from the composite LF of clusters in the 2dFGRS (de Propris et al. 2003). With an X-ray luminosity of $L_X = 7.3 \times 10^{44}$ erg/s (Ebeling *et al.* 1998), the Coma cluster is a couple of orders of magnitude more luminous than our brightest GEMS group (see Table 1).

The Leo I group is a well-known nearby ($v \sim 950$ km s $^{-1}$) group of galaxies, its proximity means that it has received attention from many researchers, notably Ferguson & Sandage (1991). More recently, Flint, Bolte, & Mendes de Oliveira (2003) have probed the faint end of the R -band LF of this group down to $M_R \sim -10$. Fig. 9 shows our determination of the LF of Leo I, which agrees well with both of the above studies.

Perhaps the most striking feature of the Leo I group LF is the lack of intermediate magnitude galaxies. We fit the cumulative LF with two Schechter functions, as above for X-ray dim groups, obtaining $M^* = -14.0 \pm 0.1$ and $\alpha = -1.20 \pm 0.01$ for the faint end ($M_R > -18$). This seems to be a rather extreme analogue of the LFs of the GEMS X-ray dim groups and indeed no group X-ray emission has been detected in the Leo I group.

4 GALAXY MERGERS AND GROUP EVOLUTION

Mergers play an important role in the evolution of galaxies in groups. Once a group has formed from gravitational collapse, violent relaxation no longer plays an important role, and the system re-

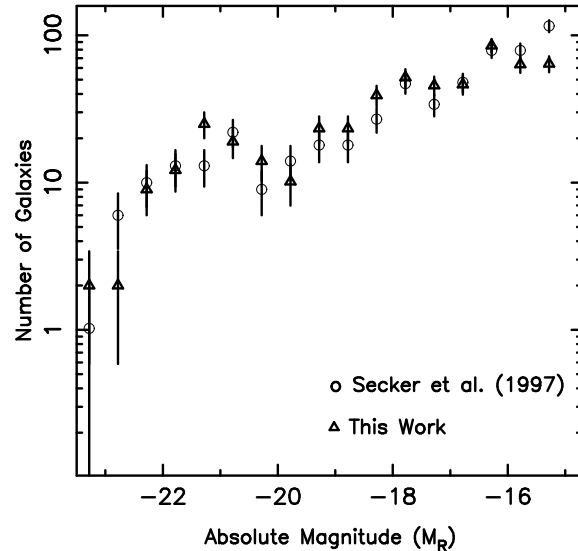


Figure 8. Differential R -band Luminosity Function for the Coma cluster. Our results are plotted alongside Secker et al. (1997) to allow direct comparison. The LF of Coma is similar to that of our X-ray bright groups, though the dip occurs in a brighter magnitude range.

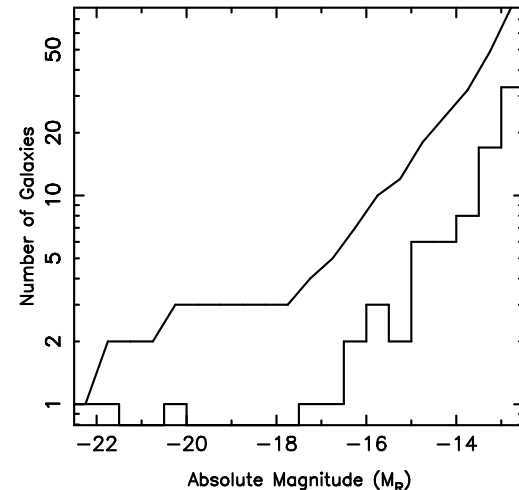


Figure 9. R -band Luminosity Function of the Leo I group. Both differential and cumulative LFs are plotted. The LF of Leo I, which hasn't been detected in the X-ray, is similar to that of our X-ray dim groups.

laxes thereafter predominantly through two-body interactions. Dynamical friction causes galaxies to fall towards the centre of the group, and together with time-dependent tidal forces, help to redistribute the ordered orbital kinetic energy, allowing the galaxies to merge. Since the deceleration due to dynamical friction is inversely proportional to the square of the relative velocity of the interacting galaxies, it is more likely to be effective in those groups with low velocity dispersion.

Here we have categorised groups according to their X-ray luminosity, since there are too few known galaxy redshifts for most of the sample groups to allow reliably measuring their velocity dispersion. Since there is a power-law relation between L_X and σ (Helsdon & Ponman 2000), we have assumed our X-ray dim groups to be of lower velocity dispersion than the X-ray bright groups. Qualitatively, therefore, we can suggest a link between merger-driven evolution and the velocity dispersion of the group,

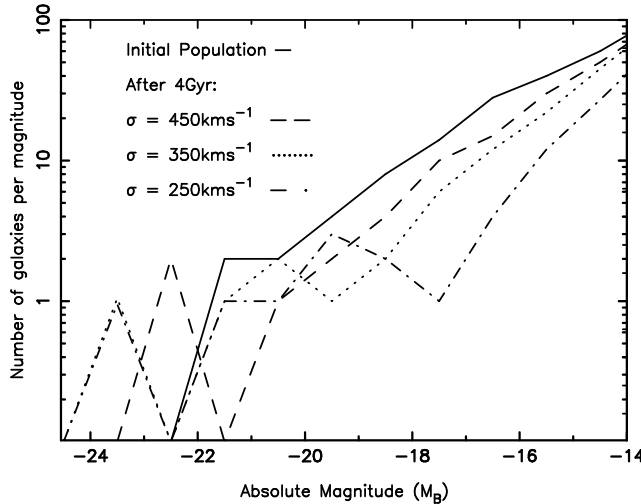


Figure 10. The shape of the differential luminosity function of the group, according to our toy model described in Section 4, after a period of 4 Gyr, starting from 50 galaxies distributed according to the luminosity function shown (solid line), for groups of one-dimensional velocity dispersion $\sigma_e = 250, 350$ and 450 km/s. Note that a dip appears at intermediate luminosities ($-18 < M_B < -16$) for the lowest σ_e group.

to explain the development of the bimodal shape of the LF in X-ray dim groups, where mergers are more likely.

To examine the role of mergers in the long-term evolution of the group luminosity function more quantitatively, we construct a toy model of a group, starting with 50 galaxies with spherical haloes, drawn from the initial luminosity function shown in Fig 10, assumed evenly distributed within a radius of $R = 1$ Mpc. A fixed mass-to-light ratio is assumed, so that mass scales simply with luminosity. The distribution of mass within each galaxy is assumed to follow a Plummer model, and the internal velocity dispersion of each galaxy is calculated from the Faber-Jackson relation $\sigma_i = 220(L/L^*)^{0.25}$ km/s (Binney & Merrifield 1998).

We follow Makino & Hut (1997) in calculating the rate of merger of pairs in this ensemble, which varies as $R_V^{-3} r_h^2 \sigma_i^4 \sigma_e^{-3}$, where r_h is the half-mass radius of each galaxy (taken to be $0.77 R_V$ for a Plummer model), and σ_i and σ_e the one-dimensional velocity dispersion of each galaxy and the group respectively. This derivation assumes that the group is in dynamical equilibrium, and that velocities of galaxies within it follow a Maxwellian distribution. Following the prescription of Makino & Hut (1997), we apply a correction factor of 0.25 to the merger rate to account for a finite limit of the binding energy of a galaxy for tidal disruption.

Now here is why we call the model we use a “toy” one. Since the Makino & Hut (1997) merger rate applies to galaxies of identical mass, we calculate the merger rate separately in each luminosity bin (i.e. we allow only for mergers of equal mass galaxies). This exercise is merely meant to examine how fast galaxies of various luminosities merge, and whether the bimodal nature can develop preferentially in low-dispersion systems.

As two galaxies merge, the light is re-distributed according to the galaxy mass. After a period of evolution T , the new galaxy magnitudes are estimated, the LF plotted and the merger rate of the new population calculated. Fig. 10 shows the result after $T = 4$ Gyrs for three different groups of one-dimensional velocity dispersion $\sigma_e = 250, 350$ and 450 km/s respectively. The lower the velocity dispersion of the group, the higher the evidence of evolution, par-

ticularly in the formation of a few galaxies at the bright end of the LF.

Fig. 11 shows the evolution of the differential LF of three groups, of one-dimensional velocity dispersion $\sigma_e = 250, 350$ and 450 km/s respectively, after time steps $T = 1, 2$ and 4 Gyrs, according to the same model. Even though we do not expect this model to be a realistic representation of a real group, this simulation does illustrate an important point. As time goes by, the faint end of the luminosity function remains featureless, while at the bright end, one or two very bright galaxies develop in the low-dispersion systems like the ones illustrated in Fig. 11, at the cost of intermediate-luminosity galaxies, which leads to the formation of a dip at these luminosities. This effect is more prominent for the lower- σ_e systems, where dynamical friction is expected to be more effective in ensuring that galaxies fall towards the centre of the group potential, as well as facilitating galaxy interactions and mergers.

We also note that in this formalism, only mergers between equal-mass galaxies are considered. A more realistic model would tend to enhance the effect of differentiation between the low-mass and high-mass galaxies, since the probability of merger between a high-mass and low-mass galaxy would be higher than that between two low-mass ones, and the bright end of the LF would be progressively enhanced as a result of mergers.

5 DISCUSSION AND CONCLUSIONS

As the exercise with the toy model in the previous section illustrates, if one starts with a Schechter luminosity function and lets a group evolve with time, the LF does not appear to evolve uniformly as dwarfs merge to form brighter and larger galaxies, but a number of factors have the potential to alter the total group LF over time.

Observations of dwarf galaxies in our local neighbourhood, particularly in the Local Group, shows us that dwarf ellipticals and spheroidals are preferentially clustered around the brighter galaxies. Statistical analyses of the distribution of satellites around giant galaxies (Lorrimer *et al.* 1994; Loveday 1997) indicate that faint companions are more strongly clustered about the primary galaxy than their brighter counterparts.

The collision time for galaxies in a group is proportional to R^{-2} , where R is the radius of a spherical galaxy. Galaxies vary widely in size; for a galaxy with absolute magnitude $M_B = -18$, a spiral would typically have $R \sim 20$ kpc, whereas an elliptical $R \sim 5$ kpc (Carroll & Ostlie 1996). The faint end of the LF is dominated by dwarf ellipticals and spheroidals that are less likely to merge with each other than bright or intermediate luminosity spirals. Indeed, we would expect the merger of a dwarf satellite with its parent bright galaxy to be a more likely event than two dwarfs merging to form an intermediate luminosity galaxy. In the Local Group (an X-ray dim group), there is direct evidence of this happening with satellites of our galaxy. The Sagittarius dwarf galaxy, for example, is in the process of being accreted by the Milky Way (Ibata *et al.* 1994), and indeed there is evidence of streams across the sky consisting of remnants of satellites being tidally torn apart by the Milky Way in the process of eventual mergers (Lynden-Bell & Lynden-Bell 1996).

As the low-mass dwarfs merge with the high-mass galaxies, we can expect the shape of the faint end of the total group luminosity function to retain its initial shape as the group evolves. The bright end of the LF in groups and clusters, on the other hand, can be expected to be modified as the brightest galaxies grow in luminosity due to mergers between the brighter galaxies, and

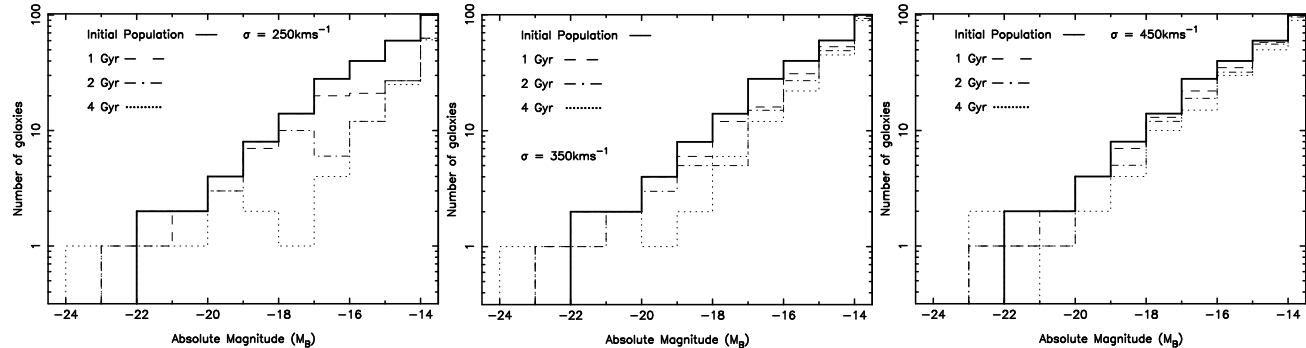


Figure 11. The evolution of the luminosity function of a group of galaxies, according to the toy model described in Section 4, after 1 Gyr, 2 Gyr and 4 Gyr, for groups with velocity dispersion $\sigma_e = 250$ (Left panel), 350 (Middle) and 450 km/s (Right panel). The growth of the bright end of the LF is more rapid in the lower σ_e group.

the intermediate luminosity galaxies get depleted. This will happen preferentially in systems of lower velocity dispersion, where mergers are more frequent, as evidenced in the observations of X-ray dim groups (Fig. 2). In the field, where mergers are rare, the intermediate-luminosity dip in the LF is not expected to appear, which is indeed the case (e.g. Madgwick et al. 2002).

Further circumstantial support for this hypothesis comes from the observations of the distribution of light in groups. Figs. 6 & 7 show that the light of the X-ray dim groups is dominated by one or two central bright galaxies, and in general the light distribution is more centrally peaked than in X-ray bright groups. This is what one expects from an evolutionary scenario illustrated in Fig. 11, where dynamical friction causes galaxies to fall towards the the centre of the group, where the rapid merger of intermediate-luminosity galaxies form the brightest central galaxies, while the faint end of the LF shows no appreciable change in slope.

We also find that the X-ray dim groups, where we see the most prominent dips in the LF, tend to contain a lower fraction of early-type galaxies, and to have less luminous Brightest Group Galaxies (Khosroshahi et al. 2004, BGG), than the X-ray bright groups. This appears to imply either (a) many of the early-type galaxies in the X-ray bright groups did not result from galaxy mergers, or (b) the merger process which has resulted in the high early-type fraction in these X-ray bright groups did not produce a LF dip, or (c) the dips in the LFs of the brighter groups have been filled in in some way. It is difficult to imagine processes that would lead to (c), and (a) is rather unlikely given that X-ray bright groups tend to have the most massive early-type BGGs.

The lack of X-ray emission in some of the X-ray dim systems could well mean that they are yet to form virialised entities, in which case they are late-forming systems, which are only now reaching a state of high density. The most likely interpretation of the shape of our LFs thus seems to be that in the X-ray dim systems, most of the galaxy mergers that are responsible for the dip in the LF have taken place in the recent past. In contrast, the X-ray bright, high- σ systems are probably not undergoing much merging at all right now (due to the high galaxy velocities), so the mergers which have affected their morphological mix and LF, will have taken place at earlier epochs, quite probably in a variety of structures which have since merged to form the group we see now. The process of merging in a variety of different precursor systems, over a range of epochs (having a range of galaxy densities) would lead to a very diverse set of contributions to the aggregate LF, which would then be unlikely to show a coherent dip.

That rich clusters of galaxies in general do not have bimodal LFs of this kind is clear from the composite cluster LFs found by de Propris et al. (2003) from the 2dF galaxy redshift survey. In the light of our model, and of the lack of strong dips in the LFs of high L_X groups, what are we to make of the presence of such dips in a minority of rich clusters, such as the Coma cluster (Fig. 8)? Clearly if one were to create a cluster by merging a set of X-ray dim groups, such as those in our sample, the result would be a cluster with a dip in the LF as seen in Coma. It therefore seems likely that the diversity in the LFs of richer clusters reflects a diversity in their formation history. Close study (White, Navarro, Evrard, & Frenk 1993) has shown Coma to be a rather unusual cluster, which shows evidence for a turbulent recent history involving multiple subcluster mergers. We speculate that clusters with strong LF dips may have been assembled primarily from multiple mergers of low velocity dispersion groups.

The results presented in this paper suggest that the low- L_X groups are sites of recent dynamical evolution. Their high- L_X counterparts, may have gone through this stage in the past with the luminosity function evolving such that the intermediate-luminosity galaxies are gradually depleted and one or two bright central galaxies form from their merger. The intermediate-luminosity bins may then be re-filled through filamentary infall.

This picture of galaxy evolution evolution leads to a definite prediction. If groups of low velocity dispersion are indeed systems that are undergoing rapid dynamical evolution, the stellar populations in their galaxies would be significantly younger than those in high- σ groups in case of dissipative merging. This can be observationally verified using sophisticated techniques to determine age without significant ambiguities from the effects of metal abundance (e.g. Nolan et al. 2003; Terlevich & Forbes 2002).

The above scenario seems to be supported by Fig. 12, which shows the relation between the X-ray luminosity of our groups and the difference in magnitude between their brightest and second brightest galaxies. The X-ray bright groups have several galaxies of comparable luminosity (and mass) at the bright end, being the end-products of earlier mergers on smaller scales in sub-groups that were incorporated in the virialised systems we observe today.

ACKNOWLEDGEMENTS

Thanks to Ale Terlevich for his involvement in observing and data reduction, John Osmond for his work on the GEMS catalogue and Habib Khosroshahi for useful discussions. VKP and PG would like

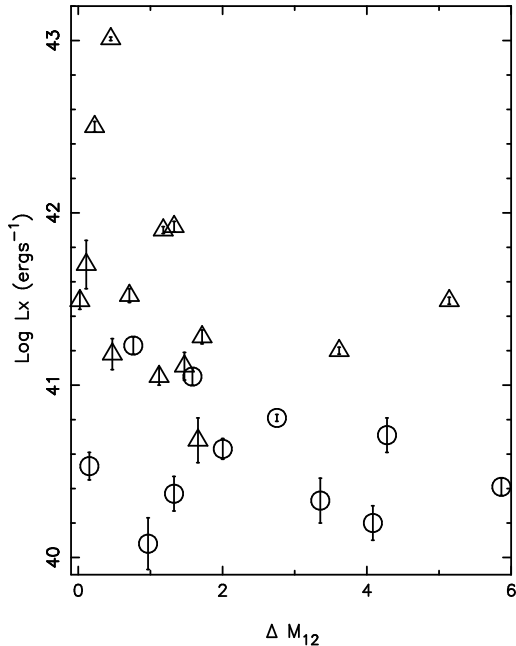


Figure 12. The X-ray luminosity of our sample groups, as a function of the difference ΔM_B between the absolute blue magnitudes of the brightest and second brightest galaxies. Groups with detected X-ray emission associated with the group, and not just with individual galaxies (see Table 1) are plotted as circles. Groups with lower L_X have systematically higher ΔM_B .

to thank the director of STScI for financial support through the Director's Discretionary Research Fund. This paper is based upon observations collected at the Issac Newton Telescope, La Palma (Observing Programme I/00A/23) and observations gathered at the European Southern Observatory, Chile (Observing Programme 67.A-0252(A)). This research has made use of the NASA/IPAC Extragalactic Database (NED) which is operated by the Jet Propulsion Laboratory, California Institute of Technology, under contract with the National Aeronautics and Space Administration.

REFERENCES

Andreon, S. & Cuillandre, J.C., 2002, *ApJ*, 569, 144
 Andreon, S. & Pello, R., 2000, *A&A*, 353, 479
 Beijersbergen, M., Hoekstra, H., van Dokkum, P.G. & van der Hulst, T., 2002, *MNRAS*, 329, 385
 Bertin, E. & Arnouts, S., 1996, *A&AS*, 117, 393
 Bernstein G.M.; Nichol, R.C.; Tyson, J.A.; Ulmer, M.P. & Wittman, D., 1995, *AJ*, 110, 1507
 Benson A.J., Bower R.G., Frenk C.S., Lacey C.G., Baugh C.M. & Cole, S., 2003, *ApJ*, 599, 38B
 Binney, J. & Merrifield, M., 1998, *Galactic Astronomy*, Princeton University Press, Princeton NJ
 Lobo C., Mazure A. & Slezak E., 1995, *A&A*, 297, 610
 Carroll, B.W. & Ostlie D.A., 1996, *Modern Astrophysics*, Addison-Wesley, New York
 Cole, S., Aragon-Salamanca A., Frenk C.S., Navarro J.F. & Zepf S.E., 1994, *MNRAS* 271, 781
 de Propris R. et al. 2003, *MNRAS*, 342, 725
 Ebeling, H., Edge, A. C., Boehringer, H., Allen, S. W., Crawford, C. S., Fabian, A. C., Voges, W. & Huchra, J. P., 1998, *MNRAS*, 301, 881
 Ferguson, H.C. & Sandage, A.R., 1991, *AJ*, 101, 765
 Flint, K., Bolte, M. & Mendes de Oliveira, C. 2001, *ApJS*, 134, 53
 Flint K., Bolte M. & Mendes de Oliveira C., 2003, *Ap&SS*, 285, 191
 Fukugita, M., Shimasaku, K. & Ichikawa, T., 1995, *PASP*, 107, 945
 Ibata, R.A., Gilmore, G. & Irwin, M.J., 1994, *Nature*, 370, 194
 Helson, S.F. & Ponman, T.J., 2000, *MNRAS*, 319, 933
 Hunsberger, S., Charlton, J. & Zaritsky, D. 1996, *ApJ*, 462, 50
 Jerjen, H., 2001, *Encyclopedia of Astronomy and Astrophysics*, McMillan, Bristol
 Jones, H. & Valdes, F. 2000, ESO Document number 2p2-MAN-ESO-22200-00002
 Kauffmann G., Colberg J.M., Diaferio A. & White, S.D.M., 1999, *MNRAS*, 303, 188
 Khosroshahi H., Raychaudhury S., Ponman T.J., Miles T. A. & Forbes D. A. 2004. *MNRAS*, in press (astro-ph/0312292)
 Madgwick, D. S., et al. 2002, *MNRAS*, 333, 133
 Landolt, A.J., 1992, *AJ*, 104, 340
 Lin, H., Kirshner, R. P., Shectman, S. A., Landy, S. D., Oemler, A., Tucker, D. L. & Schechter, P. L., 1996, *ApJ*, 464, 60L
 Lobo, C., Biviano, A., Durret, F., Gerbal, D., Le Fevre, O., Mazure, A. & Slezak, E., 1997, *A&A*, 317, 385
 Lorrimer, S.J., Frenk, C.S., Smith, R.M., White, S.D.M. & Zaritsky, D., 1994, *MNRAS* 269, 696
 Loveday, J., Maddox, S.J., Efstathiou, G. & Peterson, B.A., 1995, *ApJ*, 442, 457
 Loveday, J., 1997, *ApJ*, 489, 29
 Lynden-Bell D. & Lynden-Bell R.M., 1996, *MNRAS*,
 Makino J. & Hut P., 1997, *ApJ*, 481, 83
 Mendes de Oliveira, C. & Hickson, P., 1991, *ApJ*, 380, 30
 Nolan L. A., Dunlop J. S., Jimenez R. & Heavens A. F., 2003, *MNRAS*, 341, 464
 Osmond, J.P.F. & Ponman T.J., 2004, *MNRAS*, in press (astro-ph/0402439)
 Schechter, P.L., 1976, *ApJ*, 203, 297
 Secker, J., Harris, W.E. & Plummer, J.D., 1997, *PASP*, 109, 1377
 Smith, R.M., Driver, S.P., Phillips, S., 1997, *MNRAS*, 287, 415
 Somerville, R.S. & Primack, J.R., 1999, *MNRAS*, 310, 1087
 Terlevich, A.I. & Forbes, D.A., 2002, *MNRAS*, 330, 547
 Trentham, N. & Tully, R.B., 2002 *MNRAS* 335, 712
 Turner, E. L. & Gott, J.R., 1976, *ApJ*, 209, 6T
 White, S.D.M. & Rees, M.J. 1978, *MNRAS*, 183, 341
 White, S. D. M., Navarro, J. F., Evrard, A. E., & Frenk, C. S. 1993, *Nature*, 366, 429
 White, S.D.M. & Frenk, C.S. 1991, *ApJ*, 379, 52
 Zabludoff, A.I. & Mulchaey, J.S., 2000, *ApJ*, 539, 136
 Zepf, S.E. & Whitmore, B.C., 1991, *ApJ*, 383, 542

This paper has been typeset from a *T_EX* / *L_AT_EX* file prepared by the author.